

Determination of Stress Distribution in Crane Hook by Caustic

M. Shaban¹, M. I. Mohamed², A. E. Abuelezz³, T. Khalifa⁴

Mechatronic Engineering Department, The High Institute for Engineering, 6 October City, Egypt¹

Prof., Force and Material Metrology Department., National Institute of Standards, NIS, Egypt²

Prof., Force and Material Metrology Department., National Institute of Standards, NIS, Egypt³

Prof., Mechanical Engineering Department, Shobra Faculty of Eng., Banha University, Egypt⁴

Abstract: Crane Hooks are highly liable components and are always subjected to failure due to the amount of stresses concentration which can eventually lead to its failure. To study the stress pattern of crane hook in its loaded condition, a solid model of crane hook is prepared with the help of ABAQUS software. Real time pattern of stress concentration in 3D model of crane hook is obtained. The stress distribution pattern is verified for its correctness on an acrylic model of crane hook using shadow optical method (Caustic method) set up. By predicting the stress concentration area, the shape of the crane is modified to increase its working life and reduce the failure rates.

Keywords: Caustic method, Crane Hook, Finite Element Method, Curved Beam, Stress Distribution

I. INTRODUCTION

Crane Hooks are highly liable components that are typically used for industrial purposes. It is basically a hoisting fixture designed to engage a ring or link of a lifting chain or the pin of a shackle or cable socket and must follow the health and safety guidelines [1-4]. Thus, such an important component in an industry must be manufactured and designed in a way so as to deliver maximum performance without failure. Thus, the aim of the work is to study the stress distribution pattern of a crane hook using finite element method and to verify the results using caustic method.

II. FAILURE OF CRANE HOOKS

To minimize the failure of crane hook [5], the stress induced in it must be studied. A crane is subjected to continuous loading and unloading. This may causes fatigue failure of the crane hook but the load cycle frequency is very low [6]. If a crack is developed in the crane hook, mainly at stress concentration areas, it can cause fracture of the hook and lead to serious accidents. In ductile fracture, the crack propagates continuously and is more easily detectable and hence preferred over brittle fracture. In brittle fracture, there is sudden propagation of the crack and the hook fails suddenly [7]. This type of fracture is very dangerous as it is difficult to detect.

Strain aging embrittlement [8] due to continuous loading and unloading changes the microstructure. Bending stresses combined with tensile stresses, weakening of hook due to wear, plastic deformation due to overloading, and excessive thermal stresses are some of the other reasons for failure. Hence continuous use of crane hooks may increase the magnitude of these stresses and ultimately result in failure of the hook.

All the above mentioned failures may be prevented if the stress concentration areas are well predicted and some design modification to reduce the stresses in these areas. The aim of this study is to explore the regions of high stress concentration in the Hook as an impotent engineering component.

III. METHODOLOGY OF STRESS ANALYSIS

The analysis is carried out as follows: Finite element stress analysis of an approximate model (acrylic) of a Hook is prepared 1st. To establish the finite element procedure a virtual model similar to the acrylic model is prepared in ABAQUS and the results of the numerical stress analysis are obtained. Second; experimental stress analyses verification on a sample similar to that of model is obtained by caustic method.

IV. FINITE ELEMENT ANALYSIS (FEA)

Finite element method [9,10] has become a powerful tool for numerical solution of a wide range of engineering problems. For the stress analysis of the acrylic model of crane hook the outer geometry or profile of the model is drawn in ABAQUS. It is then extruded to 6 mm to form a 3-D model of hook. Here 6 mm is the average thickness of the model. Material properties and element type are fed and the model is meshed using smart size option with the global size of the element. Loading, as presented in Fig. 1 (a), and constraint are applied to the meshed model and the finite element model is then solved. von mises stress patterns are thus obtained as shown in Fig. 1 (b). The stress concentration regions are plotted with red and yellow colors with maximum values of 34 and 23 N/mm² at inner and outer edges of the Hook.

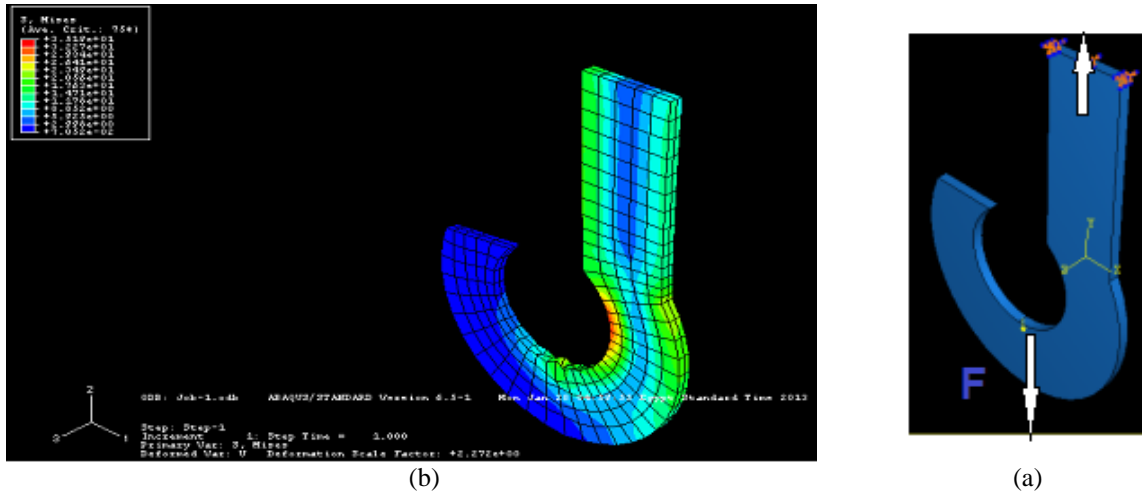


Figure 1: von mises stress in the model

V. THE PRINCIPLE OF OPTICAL METHOD OF CAUSTIC

The optical method of caustics has proved to be a powerful experimental technique to measure stress intensity factors at a crack tip in static and dynamic fracture mechanics problems, for recent examples see [11 ,12]. Due to its high sensitivity to stress gradients, the method of caustics is used in this study as a tool to provide useful information about the intensity of the stress field in the vicinity of a hole. The optical method of caustics is a technique based on geometrical optics. The method is accurate, simple and economical because the optical bench has relatively few components. The accuracy of the proposed experiments derives from the fact that the physical stress models must obey the practical laws of physics.

The principle of the method is simple in concept. The formation of the caustic image is dependent on the stresses in a structural member or machine component. Therefore, it is an ideal method to be used for when there is a stress concentration factor, since high stress gradients produce large deflections of the light rays and an image with distinguishing characteristics. The advantage of caustics relative to other optical experimental techniques is that the same equipment can be used in either, a reflection or a transmission arrangement.

The change in thickness of the specimen in plane stress condition can be obtained from generalised Hook's law, in terms of the in-plane principle stresses σ_1 and σ_2 , as:

$$\delta d = -\frac{\nu}{d}(\sigma_1 + \sigma_2)d \tag{1}$$

The stress singularity of the elastic field is transformed into optical one represented by a highly illuminated surface that contains the necessary information for determining the applied stress in this study. If a specimen that contains a central hole is loaded, the state of stress in the vicinity of the hole is much higher than the stresses along the rest of the specimen. The sum of in-plane principal stresses in the vicinity of a hole is given by Kirsch's solution [13] as:

$$\sigma_1 + \sigma_2 = \frac{\sigma}{2} (2 + 4 \frac{a^2}{r^2} \cos 2\theta) \tag{2}$$

where r and θ are the polar coordinates with the origin at the center of the hole. It is important to remember that the above equation is for infinite plate as it will be discussed in the results section.

Since σ_1 and σ_2 vary with r and θ , the front and back surfaces of the specimen deform. If a monochromatic and coherent light beam impinges on the face of transparent specimen, the deformed surfaces cause the light rays to deflect like a divergent lens. Upon transmitting and exit from the specimen, the rays are not parallel. If a screen is placed at distance Z_0 , shown in Figure 2, downstream from the specimen, the light rays produce an

interesting optical pattern, caustics. The deviation vector \mathbf{D} resulting from the light ray transmitted or reflected from the area very close to a hole in an optically isotropic medium is shown in Figure 2. The direction and magnitude of the deviation vector are correlated to the change in the optical path δs and it is given by Eikonal [14] equation as:

$$\mathbf{D} = Z_0 \text{grad } \delta s(r, \theta) \tag{3}$$

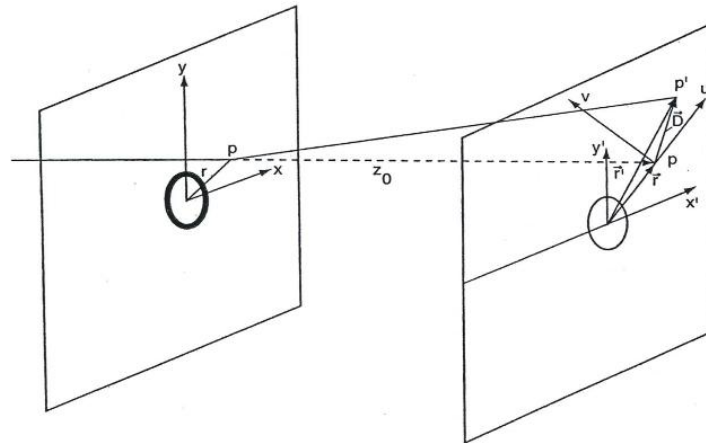


Figure 2: Development of the image equation.

Utilising the fundamentals of mirrors, the light's optical paths can be established. Consider the light ray AB that traverses the unstressed specimen as shown in Figure 3. In terms of the refractive index of the material, the initial optical path of the transmitted light is:

$$L_i = AB + nd + CD. \tag{4}$$

When a tensile stress is applied, both the thickness and refractive index of the material decrease. The final optical path of the transmitted light is equal to:

$$L_f = AB + \delta d + (n - \delta n)(d - \delta d) + CD \tag{5}$$

The change in the optical path ($L_f - L_i$) of the light, neglecting higher order term, can be calculated as:

$$\delta s = (n-1)\delta d + ds \tag{6}$$

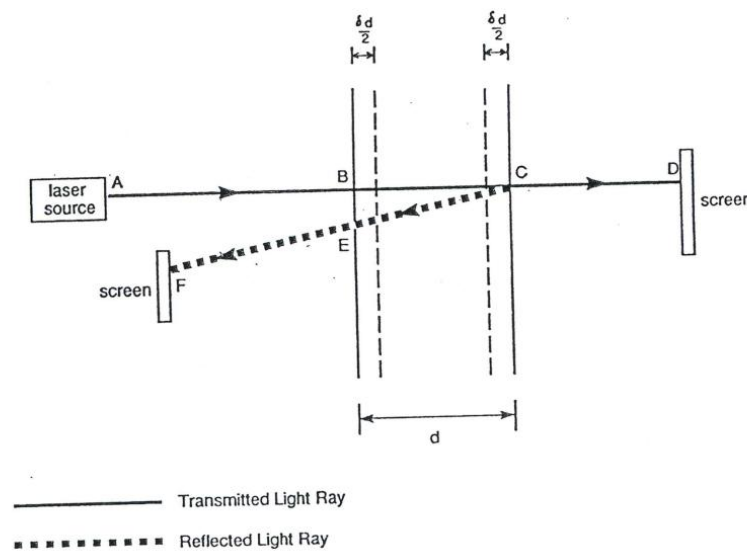


Figure 3: Optical path of light rays.

Calculus, optics and strength of materials will be linked to establish the necessary optical mechanics relationships. The change in the refractive index of isotropic material due to the in-plane principal stresses is given by Maxwell's relationship [15] as:

$$\delta n = A(\sigma_1 + \sigma_2) \tag{7}$$

If one uses Equations (1) and (7) in Equations (6), then the change in the optical path becomes:

$$\delta s = d[(1-n)\frac{v}{E} + A] (\sigma_1 + \sigma_2) \tag{8}$$

Substituting Equations (2) and (8) into Equation (3), it yields:

$$D = z_0 d\sigma \text{grad}(2 + 4\frac{a^2}{r^2} \cos 2\theta)[(1-n)\frac{v}{E} + A] \tag{9}$$

The mapping of the specimen plane on the image plane is shown in Figure 2. The point p is placed in a local region near the hole. However, after propagating down the optical bench, the deflected light ray impinges the screen at point p whose location is given by the vector r' . The image vector equation can be written as:

$$r = r + D \tag{10}$$

Substituting Equation (9) into the image Equation leads to:

$$X = r \cos \theta + 4z_0 d\sigma a^2 [(1-n)\frac{v}{E} + A] r^{-3} \cos 3\theta \tag{11a}$$

$$Y = r \sin \theta + 4z_0 d\sigma a^2 [(1-n)\frac{v}{E} + A] r^{-3} \sin 3\theta \tag{11b}$$

The caustic curve is the line between the dark shadow zone and the bright band. Therefore, the caustic is a singular curve of the image Equation (10) and the necessary condition for the existence of such singularity is when Jacobian determinant is zero [16], thus:

$$\frac{\partial x}{\partial y} \frac{\partial y}{\partial r} - \frac{\partial x}{\partial r} \frac{\partial y}{\partial \theta} = 0 \tag{12}$$

From Equations (11) and (12), a relation for the initial curve radius of the caustic on the image plane is obtained:

$$r_0 = (12 \sigma Z_0 c a^2)^{0.25} \tag{13}$$

where c is the optical constant. These relations show that the initial curve is a circle with radius r_0 [16].

Substituting the value for r_0 in Equations (11), the corresponding image equations become:

$$x = r_0 (\cos \theta + \frac{1}{3} \cos 3\theta) \tag{14a}$$

$$y = r_0 (\sin \theta + \frac{1}{3} \sin 3\theta) \tag{14b}$$

The angle θ varies between 0 and 2π . Equation (14) generate a caustic curve which can be classified as a nephroid as shown in Figure 4.

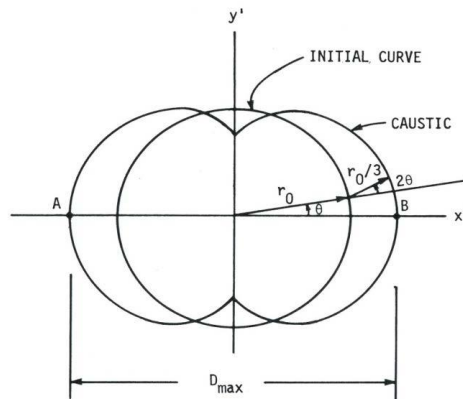


Figure 4: Theoretical initial curve and caustic

VI. EXPERIMENTAL EVIDENCE

The experimental apparatus is relatively simple. A photograph for the setup arrangements of the optical system for the experimental transmitted caustics are shown in Figure 5. Briefly, a monochromatic and coherent light beam emitted from a point source He-Ne laser, which was widened by a spatial lens, impinges normally on the specimen. The laser light beam has to be parallel. To achieve this property, the light source must have the essential features of a point source. Divergent light is used primarily to enlarge the caustic image. The direct recording of the caustic image is possible in transmission arrangements as well as in reflection arrangements. The rotation of the model produced a light beam that was not perpendicular to the specimen. This rotation created only a translation of the caustics without affecting the size, shape and relative position of the caustics. However, a rotation of the screen distorts the caustic image. Therefore, the screen should be always parallel to the model. The live caustic image can be captured by a camera.

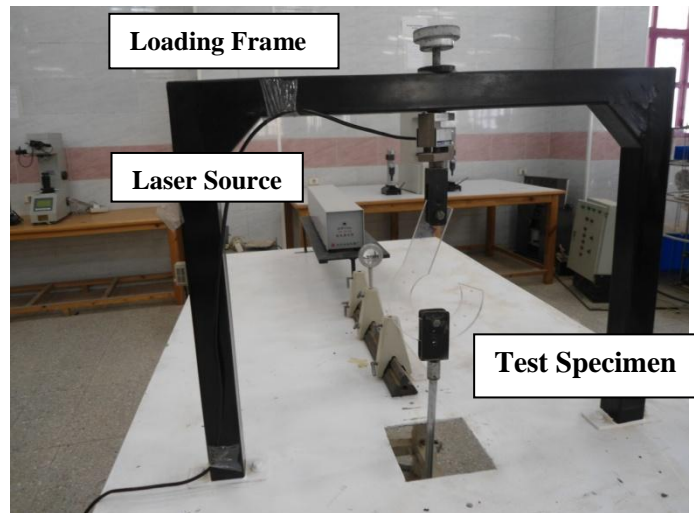


Figure 5: Experimental caustic setup

VII. TEST SPECIMEN AND CAUSTICS IMAGE

The material used is Polymethyl Methacrylate (PMMA) because it has the advantage of being a mechanically and optically isotropic material. Figure 6 show sketch for the test specimen with six distributed holes along the hook, each hole has diameter, $2R, = 3 \text{ mm}$. A transmitted light beam that impinged normally on the faces of the specimens was used. The optical set up are: $Z_o = 2050 \text{ mm}$, $Z_i = 350 \text{ mm}$, $M = 6.85$, while the material constants are $C = -1.02 \cdot 10^{-4} \text{ mm}^2/\text{N}$, $E=3000 \text{ N/mm}^2$ and the other test condition are : $F = 750 \text{ N}$, and $d = 6 \text{ mm}$. The definitions of all symbols are given afterward in notation.

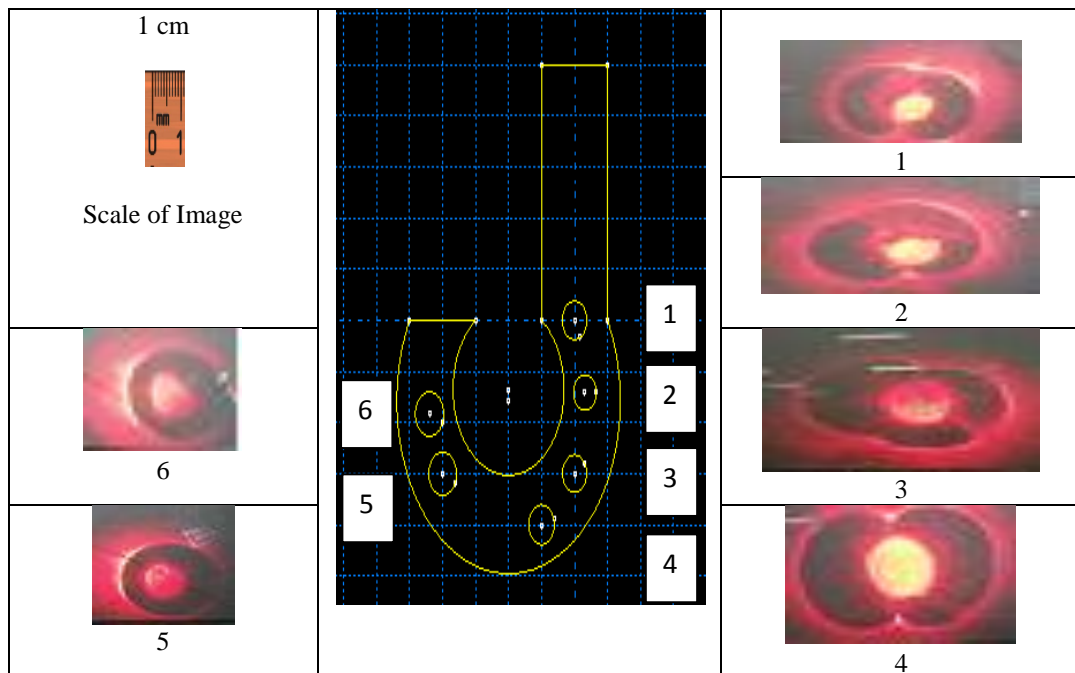


Figure 6: Caustic image for each hole on the hook specimen

The obtained caustic images (1-6) are also shown in Figure 6. Each caustics image is related to the state of stress around hole of a same number on specimen sketch (1-6). The pattern of regions is related to stress concentration as it describes the gradient of the sum of the in-plane stresses, Equation (2). The kidney shape means high stress and the circle shape means low stress. The first four holes from fixed end of the hook have kidney shape and the last two holes have circle shape.

Relation (13) shows that the radius, which defines the envelope of the highly stressed zone of the specimen, is constant. Within the framework of linear elasticity, it should be observed that the deformed shape of the specimen surface near the hole (stress concentration) is proportional to the applied stress. Thus, the light patterns obtained from the specimen surface near the hole provide a direct measure of the applied stress.

VIII. RESULTS

The maximum diameter of the caustic and the radius r_0 of the initial curve are shown in Figure 4. The maximum diameter, D_{max} is related to r_0 by Reference [17]:

$$D_{max} = 2.67 r_0 \tag{15}$$

The need for the use of the method of caustics to measure the applied load in polymeric members is discussed in Reference [18]. Substituting Equation (15) into the initial curve equation leads to:

$$\sigma = \frac{D_{max}^4}{610 z_0 c a^2 d M^3} \tag{16}$$

Equation (16) represents the basic relationship underlying the proposed optical method of measuring the stress. It is clear that the applied axial stress can be determined simply by measuring the maximum diameter of the image since d , a , c , Z_0 , and M are known parameters in a typical experiment. This experimentally applied stress is compared to the FEA. Some of the results obtained are shown in Table 1.

Table1
Comparison between FEA and experimental results

Hole number	Caustic diameter (D_{max}),mm	Optical stress (N/mm ²)	FEA stress (N/mm ²)
1	48	9.59	8.85
2	50	11.29	11.7
3	50	11.29	11.7
4	48	9.59	8.85
5	40	4.62	2.99
6	40	4.62	2.99

By observing the caustic image, one can determine the region that is affected by the presence of stress concentration. The difference between the experimental and FEA stresses as shown in figure 7 is due to the limitation of the theory of elasticity resulting from the infinite plate solution. It is clearly seen from the results at table 1 and figure 6 that the values of stresses obtained by the two methods are very close at the relatively high level of stresses. On the other hand it is expected for low level of stresses the caustic shapes tend to be circles which may lead to erroneous results.

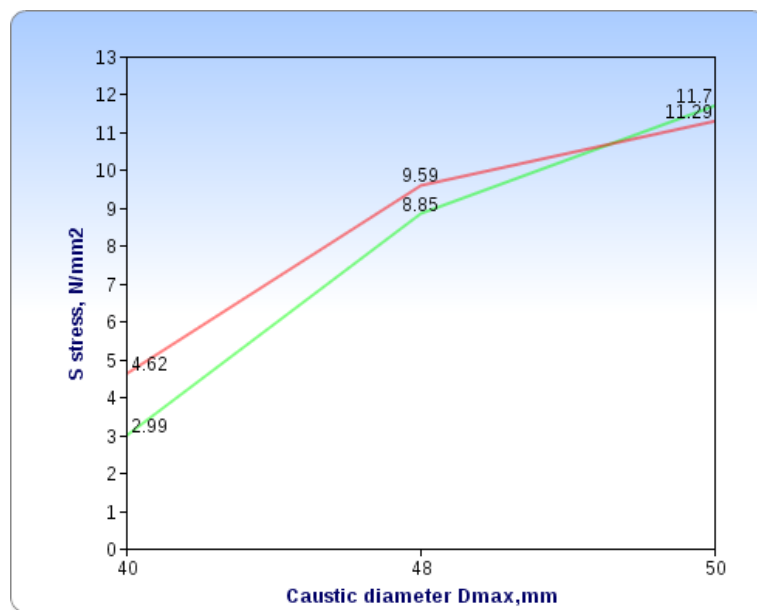


Figure 7: The variation of FEA and experimental stress versus maximum diameter of caustic

IX. CONCLUSIONS

The complete study is an initiative to establish a FEA procedure, by validating the results, for the measurement of stresses. For reducing the failures of hooks the estimation of stresses, their magnitudes and possible locations are very important. From the stress analysis we have observed the cross section of max stress area. If the area on the inner side of the hook at the portion of max stress is widened then the stresses will get reduced. The caustic method is very powerful method to detect the stress distribution for complicated mechanical elements such as hooks. By drilling several distributed small holes on the hook, the caustic method can predict accurately the stress value at each hole position. Only at the high stress levels.

NOTATIONS

- R hole radius
- C Stress optical constant
- d thickness of specimen
- D_{max} caustic's maximum diameter
- E modulus of elasticity
- F applied load
- L_i initial light path
- L_f final light path
- M magnification factor
- n refractive index
- r_o radius of initial curve
- v Poisson's ratio
- Z_i distance between the divergent light source and the model
- Z_o distance between model and screen
- W Plate width
- σ applied stress

REFERENCES

- [1] ASME Standard B30.2, "Overhead Gantry Cranes (Top Running Bridge, Single or Multiple Girder, Top Running Trolley Hoist)," 2005.
- [2] ASME Standard B30.9, "Slings Safety Standard for Cables, Blewys, Cranes, Derricks, Hoists, Hooks, Jacks and Slings," 2006.
- [3] ASME Standard B30.10, "Hooks Safety Standard for blewys, Cranes, Derricks, Hoists, Hooks, Jacks and Slings," 2009.
- [4] Department of Labour of New Zealand, "Approved Code of Practice for Cranes," 3rd Edition, 2009.
- [5] B. Ross, B. McDonald and S. E. V. Saraf, "Big Blue Goes Down. The Miller Park Crane Accident," *Engineering Failure Analysis*, Vol. 14, No. 6, pp. 942-961, 2007.
- [6] Fatigue cycles <http://www.public.edu>
- [7] J. Petit and D. L. Davidson, "Fatigue Crack Growth Under Variable Amplitude Loading", Springer Publisher, New York, 2007.
- [8] Y. Yokoyama, "Study of Structural Relaxation- Induced Embrittlement of Hypoeutectic Zr-Cu- Al", *Ternary Bulk Glassy Alloys*, *Acta Materialia*, Vol. 56, No. 20, pp. 6097-6108, 2008.
- [9] S. S. Bhavikatti, "Finite Element Analysis," New Age International, New Delhi, 2007.
- [10] P. Seshu, "Textbook of Finite Element Analysis", PHI Learning Pvt. Ltd., New Delhi, 2004
- [11] M. Shaban, M. I. Mohamed, A. Abu El Ezz and M. G. El Sherbiny, "Stress Distribution in Crack-Craze Region Using Caustic Method for Polymeric Materials with Different Agents", *ASJME*, vol. 1, April, pp. 35-41, 2010.
- [12] Gong, K. and Li, Z., "Caustics Method in Dynamic Fracture Problem of Orthotropic Materials", *Optics and Lasers in Engng.*, 46, 8, pp. 614-619, 2008.
- [13] Riley, W.F., Sturges, L.D. and Morris, D.H., *Mechanics of Materials*, (6th Edn), John Wiley, 2007.
- [14] Born, M. and Wolf, E., *Principles of Optics*, (7th Edn), New York: Pergamon Press, 2002.
- [15] Feisel, L.D. and Rosa, A.J., "The Role of the Laboratory in Undergraduate Engineering Education.", *J. of Engng. Educ.*, 94, 1, pp. 121-130, 2005.
- [16] M. Shaban, A. Abu El Ezz and M. G. El Sherbiny, "Stress Distribution In Craze Region Using Caustic Technique In Polymeric Materials", Master thesis, Cairo university, 2008.
- [17] Papis, D.N., Agioutantis, Z. and Kourkoulis, S.K., "The Optical Method of Reflected Caustics Applied for a Plate with a Central Hole: Critical Points and Limitations", *Strain*, 47, 2, pp. 1-10, 2011.
- [18] Younis, N.T., "New Optical Method for Determining Poisson's Ratio/Young's Modulus for Transparent Materials", *Optical Engng.*, 41, 2, pp. 471-478, 2002.